CARBON 50 (2012) 5458–5462

Available at www.sciencedirect.com

SciVerse ScienceDirect

journal homepage: www.elsevier.com/locate/carbon

Phase transitions in single crystal tubes formed from C_{60} molecules under high pressure

J.Y. Hu [a,b], N.N. Niu [c], G.Z. Piao [c], Y. Yang [a], Q. Zhao [b], Y. Yao [a], C.Z. Gu [a], C.Q. Jin [a], R.C. Yu [a,*]

[a] Beijing National Laboratory for Condensed Matter Physics, Institute of Physics, Chinese Academy of Sciences, P.O. Box 603, Beijing 100190, PR China

[b] Department of Physics, School of Science, Beijing Institute of Technology, Beijing 100081, PR China

[c] Key Laboratory of Rubber–Plastics, Ministry of Education, School of Polymer Science and Engineering, Qingdao University of Science and Technology, Qingdao 266042, PR China

ARTICLE INFO

Article history:
Received 13 March 2012
Accepted 23 July 2012
Available online 31 July 2012

ABSTRACT

Pure single crystal tubes formed from C_{60} molecules, with a face-centered cubic (fcc) structure were fabricated by a liquid–liquid interfacial precipitation method using C_{60} powder. A bulk transition from fcc to a simple cubic structure and a surface transition from (1×1) to (2×2) have been observed around 246 K (bulk transition temperature T_B) and 214 K (surface transition temperature T_S), respectively, during the measurement of the temperature dependence of electrical resistance. The initiation of the two transitions under pressure was investigated using a piston cylinder high pressure apparatus and it was found that both T_B and T_S increase with increasing pressure. And the C_{60} molecules at the surface of the tube exhibit the same behavior of that in the bulk at a pressure of about 2.1 GPa.

1. Introduction

Due to its unique physical and chemical characteristics, C_{60} has been extensively studied since its discovery [1]. At room temperature, the C_{60} crystal has a face-centered cubic (fcc) structure ($Fm\bar{3}m$) with $a = 14.2$ Å and undergoes a first order phase transition to a simple cubic (sc) structure ($Pa\bar{3}$) at around 250 K [2–5]. This transition is called bulk transition and it is characterized that the fcc lattice has an orientational disorder while the sc has an orientational order. The sc phase is realized by the forming of inequivalent orientations of the four molecules in the fcc cell without any lattice distortion or molecular displacements [2,3]. Using the electron energy-loss spectroscopy (EELS) and low-energy electron diffraction (LEED), Goldoni et al. [6] reported that this bulk phase transition is associated with a surface counterpart, a transition from (1×1) to (2×2) in symmetry of the (111) surface at around 225 K, about 30 K lower than the temperature of the bulk transition. The calculations by Laforge et al. [7] suggest that there is a two-stage rotational disordering in C_{60} molecular crystal surface. One molecule in the (2×2) surface unit cell has significant different orientation from the other three molecules, making it more frustrated, and its thermal-activated rotational behavior differs from that of the others. So the surface thermal rotational disorder undergoes an intermediate regime that the more frustrated molecule becomes disordered much earlier than the other three molecules, which also lose their rotational order at 230 K. And Goldoni et al. [8] provided strong experimental evidences for this partial disordered intermediate regime by high resolution core level photoemission. In addition, when temperature decreases to about 90 K, a phase transition called as glass transition happens [9]. These phase transitions were confirmed by Kumar et al. [10] in C_{60} thin films by temperature dependent electrical transport measurements.

* Corresponding author.
E-mail address: rcyu@aphy.iphy.ac.cn (R.C. Yu).

0008-6223/$ - see front matter
http://dx.doi.org/10.1016/j.carbon.2012.07.032

Recently, fullerene nanomaterials have attracted attention for their importance in both fundamental research and potential applications in nanoscale devices. Wang et al. reported the synthesis of C_{60} sheets and suggested that C_{60} crystals in even small size will be a potential candidate of superhard materials [11]. C_{60} rods with nano- and submicro-meter dimensions were polymerized under high pressure and high temperature conditions and were indexed to a rhombohedral polymeric structure [12]. Liu et al. fabricated nanowires and nanotubes from C_{60} by the dipping porous alumina templates into a solution containing C_{60} [13], but the tubes were polycrystalline and had a mixture of face-centered cubic and hexagonal close-packed phases. Later, a modified liquid–liquid interfacial precipitation (LLIP) method was used to fabricate pure fullerene nanotubes (pure fullerene nanowhiskers with hollow structures) [14–17], which are single crystal and have an fcc structure after being fully dried at room temperature. These tubes, known as C_{60} nanotubes, with diameters smaller than 1000 nm and several millimeters in length, could be re-dissolved in appropriate solvents, so they may be useful not only as adsorbents and catalysts but also as templates for the various forms of materials such as fibers and membranes [17].

To design and optimize the properties of the nanodevices made of nanotubes and nanowires, it is essential to study the electronic properties of their building blocks: individual nanotube and nanowire. Recently, the intrinsic electronic transport properties of individual nanowires have been explored by using focused ion beam (FIB) technique and four-probe electrical measurement [18,19]. As well known, the physical properties of a material are determined by its structure. High pressure, as a new dimension, can tune the crystal structures and electronic structures of materials and further their physical properties. Molecular crystals such as C_{60} materials are very sensitive to high pressure since the intermolecular bonds in them are easily compressed and the molecules themselves may also be modified under pressure [20,21]. In our previous work [22], we have reported the amorphization and isostructural phase transition of C_{60} nanotubes induced by high pressure. Here, we report the temperature dependence of electrical resistivity in a single C_{60} nanotube and the evolution of phase transition temperature under pressure up to 2.4 GPa.

2. Experiments

The C_{60} nanotubes are fabricated by the LLIP method. As reported elsewhere [14–16,22], the pristine C_{60} powder (MTR Ltd. 99.5%) was dissolved in pyridine, and then the pyridine solution of C_{60} was added to isopropyl alcohol in a proper mixture ratio. One minute ultrasonic dispersion was taken to obtain suitable diffusion at the interface. In order to promote the growth of the C_{60} nanotubes, the solutions were exposed to visible light such as blue light with a center wavelength of 468 nm. The hollow structure of the C_{60} nanotubes was characterized using transmission electron microscope (TEM, JEM-2000EX). In the TEM experiments, the specimens were placed on a copper micro grid with carbon film.

The C_{60} nanotubes were spread on a silicon oxide surface and an appropriately isolated one was identified by a scanning electron microscope. Then two pairs of Pt microleads typically 500 nm in width and 100 nm in thickness were fabricated by FIB deposition (Dual-Beam 235 FIB System from FEI Company, the working voltage of the system was 5 kV for the electron beam and 30 kV for the focused ion beam, respectively, and the current of the focused ion beam was $50 \sim 500$ pA), as shown in Fig. 1(b). Finally, the electrical connection between the Pt microleads and the sample holder was made by highly conductive silver paste and Pt wires.

The measurements of temperature-dependent resistance curves R(T) under hydrostatic pressures up to 2.4 GPa were carried out by using the four-probe technique in a piston cylinder pressure cell, with a 1:1 mixture of silicon oil and coal oil as pressure transmitting medium. The pressures were loaded at room temperature.

3. Results and discussion

Fig. 1(a) shows a typical hollow image of the C_{60} nanotube, the tubular structure is clearly revealed, and the diameters of the sample are smaller than 1000 nm with the lengths exceeding several micrometers. Most of the nanotubes have a width of 200–500 nm, and those with diameters smaller than 200 nm seldom show tubular structure, this means a moderately large diameter is needed for the formation of C_{60} fullerene nanotubes fabricated by LLIP [14]. A typical SEM image of four probes on an individual nanotube is shown in Fig. 1(b), the platinum microleads fabricated by FIB deposition have a good contact with the nanotube. The nanotubes have a fcc structure with a space group of Fm3 m and cell constant of $a = 1.424$ nm at room temperature [23].

Fig. 2 shows the electrical resistivity (R) as a function of temperature (T) of a single C_{60} nanotube. The measured temperature range is $120 \sim 290$ K. The features at temperatures 246 and 214 K as seen in Fig. 2 are attributed to two different transitions in C_{60} nanotube, these transitions are supposed to be designated as fcc to sc phase transition (bulk transition temperature T_B) and surface transition from (1×1) to (2×2) reconstruction (surface transition temperature T_S), respectively. As temperature decreases, the resistivity increases, while it decreases between 246 and 251 K. We suppose this change is related to the bulk transition similar to the case in a pure C_{60} single crystal where the transition happens

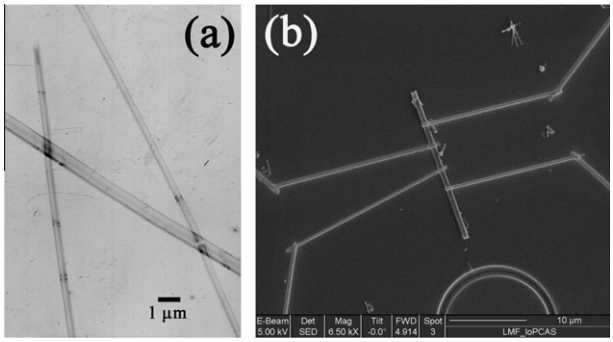

Fig. 1 – (a) TEM image of the C_{60} nanotubes, (b) typical SEM images of a single C_{60} nanotube and the attached four Pt microleads.

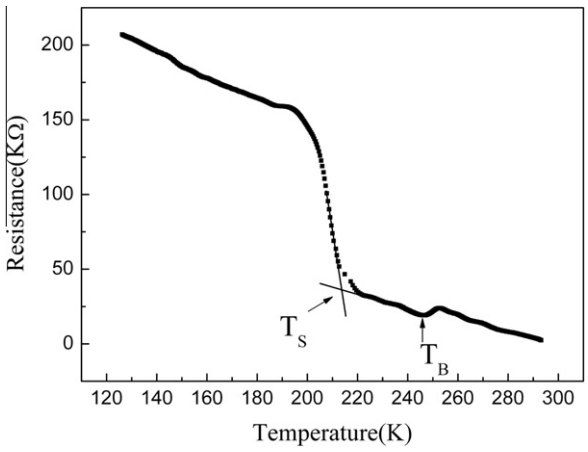

Fig. 2 – Temperature dependence of resistance R(T) for a single C_{60} nanotube.

around 250 K [2–4] accompanying a sharp increase in the conductivity when the crystal is cooled down through the bulk transition [4]. The bulk transition temperature in C_{60} nanotubes is a little lower compared with the C_{60} single crystal and this may be due to the nano-size effect. The C_{60} nanotube could exhibit both bulk and surface characteristics just because its hollow structure and the nanoscale effect, we think. In C_{60} thin film, it was reported that a surface transition from (1×1) to (2×2) happens at the temperature around 225 K [6–8]. In the C_{60} nanotube, as the temperature decreases to about 214 K, 32 K lower than T_B, a huge increase of resistance happens. This is supposed to be correlated with the surface transition, and the T_S is a bit lower than that in C_{60} thin film. When the surface rearrangement from (1×1) to (2×2) happens, the number of molecules in a surface will be less and intermolecular distances become larger, which leads to anomaly in resistivity [10].

The thermally activated conductivity of the C_{60} nanotubes can be written as [24]:

$$\sigma = \sigma_0 \exp(-E/K_B T)$$

where σ is the conductivity of the C_{60} nanotube, σ_0 is the conductivity prefactor, K_B is the Boltzmann constant, T is the absolute temperature, and E is the activation energy. The activation energies of the carriers motion can be more or less accurately estimated from $(\ln\sigma^{-1})$ versus $(1/T)$. Through fitting the temperature dependence of the resistance curve, the activation energies are obtained as 0.21 and 0.17 eV, respectively, above and below the bulk phase transition temperature $T_B = 246$ K. In the literatures, the band-gap values of C_{60} crystals obtained by optical or photoemission measurements were reported to be about 1.9–2.3 eV [25,26]. Our calculated activation energies are much lower than half of the energy gap, but they are comparable to the published data [4,5,18,27,28]. The activation energies in the C_{60} bulk crystals were reported to be 0.66–0.58 and 0.35–0.38 eV above and below T_B [4,5] calculated through temperature dependence of electrical resistance, respectively. Wen et al. [5] supposed that the obviously low conduction activation energy may indicate the presence of similar midgap states in C_{60} crystal as the case of $BaBiO_3$. For $BaBiO_3$, the optical measurement indicates a gap of 2.0 eV while the electrical conductivity measurement gives the activation energy of 0.24 eV [29], the inconformity is attributed to the formation of midgap states related to the local charge density. In doped C_{60} with K, Takahashi et al. [26] observed the formation of midgap states. Moreover, Arai et al. [27] reported that the activation energy of C_{60} single crystal is 0.26 and 0.15 eV above and below T_B, respectively, which is ascribed to an impurity level. In our case, the FIB process may induce some defects to the C_{60} nanotubes at the junction, these defects could decrease the conduction activation energy. In addition, different from the bulk C_{60}, since the C_{60} nanotube has some bending structure characteristic (tubular structure), which would cause some changes of band structure, this is also one possible reason for its having different activation energies. And our results are close to that of C_{60} nanorods reported by Ji et.al [18], in which the activation energies are 0.16 eV above T_B and 0.12 eV below T_B. The lower activation energies of C_{60} nanotubes than that of bulk C_{60} indicate the easier carrier injection of C_{60} nanotube, which will be invaluable for future nanodevice fabrication.

The temperature dependences of electrical resistivity for a single C_{60} nanotube under different pressures are shown in Fig. 3(a). With increasing pressure, both T_B and T_S move to higher temperatures, and the temperature range $\Delta T = T_B - T_S$

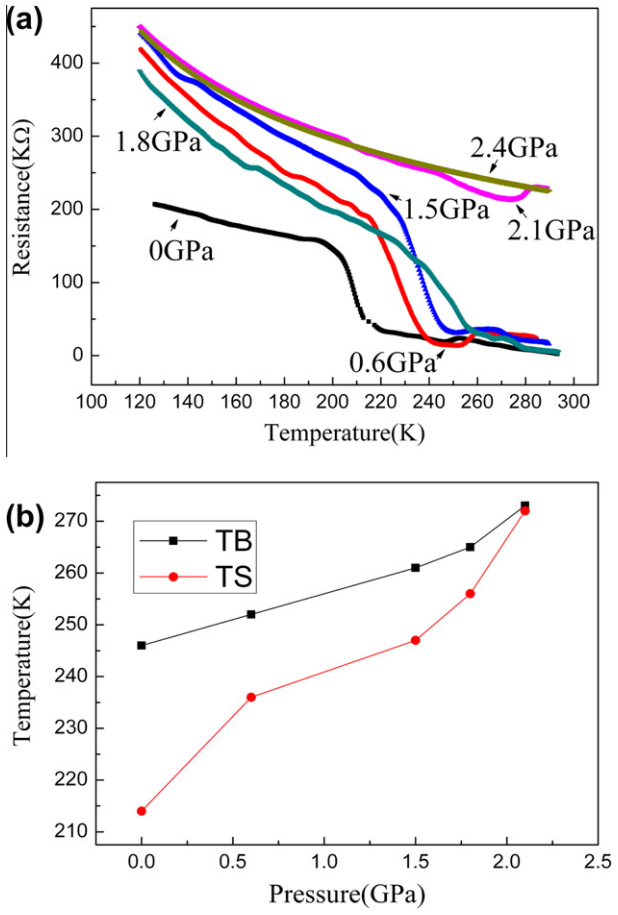

Fig. 3 – (a) The temperature-dependent resistance curves R(T) of C_{60} nanotube measured under different pressures, (b) the bulk transition temperature T_B and surface transition T_S versus pressure P.

becomes small (Fig. 3(b)). The two phase transition temperatures almost overlap to one under 2.1 GPa. When the pressure reaches 2.4 GPa, T_B and T_S could not be measurable in our experimental temperature range. It was reported that the fcc structure of bulk C_{60} crystals transforms into a sc structure as the pressure reaches 0.23 GPa [30], and Wang et al. reported that the C_{60} sheets undergo a similar transformation at a pressure of about 1.3 GPa, about 1 GPa higher than that for bulk C_{60} [11]. The pressure could facilitate the phase transition from the fcc to the sc structure in some C_{60} crystalline materials, this is consistent with the T_B increases as pressure increases. We all know that the surface properties of a solid are influenced to a large extent by the bulk properties, the surface rearrangement from (1×1) to (2×2) could be resulted from the fcc to sc bulk phase transition [6]. So the T_S exhibits a similar behavior as T_B.

Based on classical Monte Carlo simulation, Laforge et al. [7] reported that there are altogether four phases or regimes of C_{60} in the whole temperature range: a fully ordered state ($Pa\bar{3}$) below 150 K; an intermediate phase with 1/4 molecules disordered and 3/4 molecules ordered surface on a ordered bulk ($Pa\bar{3}$) between 150 and 230 K; a disordered surface layer on an ordered bulk ($Pa\bar{3}$) between 230 and 250 K; a fully rotationally disordered state ($Fm\bar{3}m$) above 250 K. In our experiments, T_S was determined as 214 K, which corresponds to the state that 3/4 molecules at the surface are ordered while 1/4 disordered. Crystal fields and intermolecular interactions compose the rotational ordering forces, and both of them at surface are different from that in bulk. As reported by Laforge et al., in fullerene, the crystal field is quantitatively very important in the bulk and its change at the surface may lead to an early thermal disordering taking place [7]. With increasing pressure, the crystal cell of C_{60} nanotube is compressed and the distance among the molecules becomes shorter, and consequently, the crystal field and intermolecular interactions are both enhanced, which favor orientational order. Hence, higher temperature would be needed to break the ordered state under pressure. In addition, in C_{60} single crystal, the sc phase with lattice constant of $a = 14.04 \pm 0.01$ Å is denser than the fcc phase with lattice constant of $a = 14.17 \pm 0.01$ Å [2], so the sc structure could be favored under high pressure. Based on above reasons, it would be reasonable that the T_B increases with increasing pressure, just as observed in our experiments. Under pressure, C_{60} molecules at surface would lose their mobility and specific surface effect, so that their behavior would trend to the bulk characteristics. In this case, the T_S would increase with pressure. It is expected that at a certain pressure all the C_{60} molecules at the surface would exhibit the same behavior of that in the bulk. In our study, this happens at a pressure of about 2.1 GPa, where T_S and T_B almost overlap to one, indicating the uniform property in the C_{60} nanotube.

Our studies show that the pressure could affect surface physical properties of functional materials through changing their structures. The individual surface property may be declined under pressure. As well known, many devices are designed based on the specific surface properties of functional materials. So high pressure effect must be considered in the practical applications of the devices in some particular environments, such as undersea operations and mining works, etc.

4. Conclusions

Pure single crystalline C_{60} nanotubes with fcc structure were fabricated by LLIP method. Two phase transitions, bulk transition and surface transition, have been observed at $T_B = 246$ K (a little lower than that in bulk C_{60} single crystal and C_{60} thin film) and $T_S = 214$ K, respectively. Calculated activation energies are 0.21 eV above T_B and 0.17 eV below T_B and lower than that of C_{60} bulk material, indicating the easier carrier injection in C_{60} nanotubes. It is found that both T_B and T_S increase with increasing pressure and they overlap to one at about 2.1 GPa, indicating the uniform property in the C_{60} nanotube.

Acknowledgements

This work was supported by the State Key Development Program for Basic Research of China (Grant No. 2012CB932302), the National Natural Science Foundation of China (Grant No. 50921091), the Program for International S&T Cooperation Projects of China (2011DFA50430), and the specific funding of Discipline and Graduate Education Project of Beijing Municipal Commission of Education.

REFERENCES

[1] Kroto HW, Heath JR, Obrien SC, Curl RF, Smalley RE. C_{60}: buckminsterfullerene. Nature 1985;318(6042):162–3.
[2] Heiney PA, Fischer JE, Mcghie AR, Romanow WJ, Denenstein AM, Mccauley JP, et al. Orientational ordering transition in solid C_{60}. Phys Rev Lett 1991;66(22):2911–4.
[3] David WIF, Ibberson RM, Matthewman JC, Prassides K, Dennis TJS, Hare JP, et al. Crystal structure and bonding of ordered C_{60}. Nature 1991;353(6340):147–9.
[4] He PM, Xu YB, Zhang XJ, Zhen XB, Li WZ. Electrical conductivity studies of a pure C_{60} single crystal. J Phys: Condens Mater 1993;5(37):7013–6.
[5] Wen C, Li J, Kitazawa K, Aida T, Honma I, Komiyama H, et al. Electrical conductivity of a pure C_{60} single crystal. Appl Phys Lett 1992;61(18):2162–3.
[6] Goldoni A, Cepek C, Modesti S. First-order orientational-disordering transition on the (1 1 1) surface of C_{60}. Phys Rev B 1996;54(4):2890–5.
[7] Laforge C, Passerone D, Harris AB, Lambin P, Tosatti E. Two-stage rotational disordering of a molecular crystal surface: C_{60}. Phys Rev Lett 2001;87(8):085503.
[8] Goldoni A, Cepek C, Larciprete R, Sangaletti L, Pagliara S, Paolucci G, et al. Core level photoemission evidence of frustrated surface molecules: a germ of disorder at the (1 1 1) surface of C_{60} before the order–disorder surface phase transition. Phys Rev Lett 2002;88(19):196102.
[9] Gugenberger F, Heid R, Meingast C, Adelmann P, Braun M, Wuhl H, et al. Glass transition in single-crystal C_{60} studied by high-resolution dilatometry. Phys Rev Lett 1992;69(26):3774–7.
[10] Kumar A, Singh F, Kumar R, Tripathi A, Avasthi DK, Pivin JC. Electrical transport study of structural phase transitions in C_{60} films and the effect of swift heavy ion irradiation. Solid State Commun 2006;138(9):448–51.
[11] Wang L, Liu BB, Liu DD, Yao MG, Yu SD, Hou YY, et al. Synthesis and high pressure induced amorphization of C_{60} nanosheets. Appl Phys Lett 2007;91(10):103112.
[12] Hou YY, Liu BB, Ma H, Wang L, Zhao Q, Cui T, et al. Pressure-induced polymerization of nano- and submicrometer C_{60}

rods into a rhombohedral phase. Chem Phys Lett 2006;423(1–3):215–9.
[13] Liu HB, Li YL, Jiang L, Luo HY, Xiao SQ, Fang HJ, et al. Imaging as-grown [60] fullerene nanotubes by template technique. J Am Chem Soc 2002;124(45):13370–1.
[14] Miyazawa K. Fullerene nanowhiskers. Singapore: Pan Stanford Publishing; 2011.
[15] Miyazawa K, Minato J, Yoshii T, Fujino M, Suga T. Structural characterization of the fullerene nanotubes prepared by the liquid–liquid interfacial precipitation method. J Mater Res 2005;20(3):688–95.
[16] Qu YT, Liang SC, Zou K, Li SX, Liu LM, Zhao JA, et al. Effect of solvent type on the formation of tubular fullerene nanofibers. Mater Lett 2011;65(3):562–4.
[17] Minato J, Miyazawa K, Suga T. Morphology of C_{60} nanotubes fabricated by the liquid–liquid interfacial precipitation method. Sci Technol Adv Mater 2005;6(3–4):272–7.
[18] Ji HX, Hu JS, Wan LJ, Tang QX, Hu WP. Controllable crystalline structure of fullerene nanorods and transport properties of an individual nanorod. J Mater Chem 2008;18(3):328–32.
[19] Long YZ, Duvail JL, Li MM, Gu CZ, Liu ZW, Ringer SP. Electrical conductivity studies on individual conjugated polymer nanowires: two-probe and four-probe results. Nanoscale Res Lett 2010;5(1):237–42.
[20] Woo SJ, Lee SH, Kim E, Lee KH, Lee YH, Hwang SY, et al. Bulk modulus of the C_{60} molecule via the tight binding method. Phys Lett A 1992;162(6):501–5.
[21] Ruoff RS, Ruoff AL. Is C_{60} stiffer than diamond. Nature 1991;350(6320):663–4.
[22] Hu JY, Liang SC, Piao GZ, Zhang SJ, Zhang QH, Yang Y, et al. Amorphization of C_{60} nanotubes under pressure. J Appl Phys 2011;110(1):014301.
[23] Minato J, Miyazawa K. Structural characterization of C_{60} nanowhiskers and C_{60} nanotubes fabricated by the liquid–liquid interfacial precipitation method. Diamond Relat Mater 2006;15(4–8):1151–4.
[24] Wang JC, Chen YF. The Meyer–Neldel rule in fullerenes. Appl Phys Lett 1998;73(7):948–50.
[25] Pichler K, Graham S, Gelsen OM, Friend RH, Romanow WJ, Mccauley JP, et al. Photophysical properties of solid films of fullerene, C_{60}. J Phys Condens Mater 1991;3(47):9259–70.
[26] Takahashi T, Suzuki S, Morikawa T, Katayama-Yoshida H, Hasegawa S, Inokuchi H, et al. Pseudo-gap at the Fermi level in K_3C_{60} observed by photoemission and inverse photoemission. Phys Rev Lett 1992;68(8):1232–5.
[27] Arai T, Murakami Y, Suematsu H, Kikuchi K, Achiba Y, Ikemoto I. Resistivity of single-crystal C_{60} and effect of oxygen. Solid State Commun 1992;84(8):827–9.
[28] Zahab A, Firlej L. Resistivity in C_{60} thin-films of high crystallinity. Solid State Commun 1993;87(10):893–7.
[29] Uchida S, Kitazawa K, Tanaka S. Superconductivity and metal-semiconductor transition in $BaPb_{1-x}Bi_xO_3$. Phase Trans 1987;8(2):95–128.
[30] Pintschovius L, Blaschko O, Krexner G, Pyka N. Bulk modulus of C_{60} studied by single-crystal neutron diffraction. Phys Rev B 1999;59(16):11020–6.